Geosciences Journal
DOI 10.1007/s12303-015-0045-y
ⓒ The Association of Korean Geoscience Societies and Springer 2016

A model-based approach for integration analysis of well log and seismic data for reservoir characterization

Atul Kumar*
Mohd Haris Mohd Khir
Wan Ismail Wan Yusoff

Department of Electrical and Electronic Engineering, Universiti Teknologi PETRONAS, Bandar Seri Iskandar, 31750, Tronoh, Perak, Malaysia
Department of Geosciences, Universiti Teknologi PETRONAS, Bandar Seri Iskandar, 31750, Tronoh, Perak, Malaysia

ABSTRACT: Accurate reservoir model requires complete information of subsurface properties, specifically porosity and permeability. Reservoir heterogeneity is the fundamental challenge for geoscientists to predict these properties which may affect the reservoir performance and their well productivity. Porosity is one of the key parameters for accumulation of hydrocarbon but its prediction is difficult due to significant variation over a reservoir volume. A spatial distribution of porosity can be investigated by integrating the 3-D seismic and well log attributes which may help in determining such reservoir variation. In addition, nonlinear multivariable regression techniques such as multivariable transform, Genetic algorithm, and Probabilistic Neural Network analysis have also been implemented to achieve high correlation coefficients between well log properties and seismic data. Results from nonlinear regression have better correlations than linear regression. In this study, a 3-D low frequency model (LFM) is proposed which can be estimated by kriging interpolation of resultant impedance values from well log data. Furthermore, "seismic inversion" is adopted for extracting correlated attributes to merge with the LFM so as to better construct a pseudo log volume. A polynomial neural network (PNN*[1]) is utilized to convert resultant acoustic impedance values into a distinct reservoir property such as porosity. PNN* is trained, tested and validated by using gamma-ray and resultant acoustic impedance values as input and effective porosity values as a target. The trained PNN* is then applied over the whole reservoir volume to generate a pseudo log volume. In the proposed low frequency model, an attempt has been made to achieve high correlation between the predicted and measured porosity logs. It will improve the reservoir characterization and lead to better estimation of hydrocarbon reserves. This low frequency model achieves better correlation between the predicted and true porosity log even with a minimum number of measured well logs.

Key words: 3-D seismic volume, seismic-well tie, probabilistic neural network, seismic inversion, reservoir characterization

1. INTRODUCTION

The current study signifies the increasing demand of accurate reservoir modelling by introducing a better numerical model based techniques to improve the reservoir characterization. The demand is required by the oil and gas industries due to economic realities: better reservoir definition using reliable technique provides higher exploration drilling success and fewer appraisal wells. Integration of available subsurface data is the key in determining better reservoir characterization. For this purpose, the mathematical approach is applied over input data to develop an integrated model (Xu et al., 1995; Balch et al., 1998). This model has significant impact over existing methodology such as multivariable transformation, genetic algorithm, linear multi-attribute transformation, probabilistic neural network, etc. which may result in higher accuracy in seismic-well tie (Specht, 1990; Oh et al., 2001; Banchs, 2002; Leiphart et al., 2002; Dorrington et al., 2004; Singh et al., 2004; Choi, 2011; Hampson, 2011; Uden, 2013). However, an error in the results is still driven to the data (well log and seismic) due to the reservoir heterogeneity. These errors must be analysed appropriately to improve the data for reservoir characterization. Therefore, an elementary process for predicting the seismic attributes with minimum prediction error is depicted in Figure 1 and

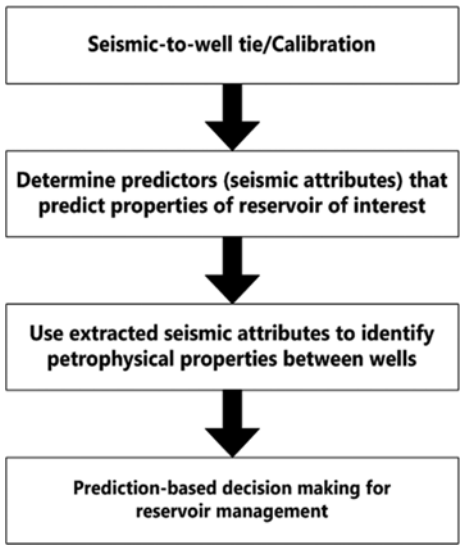

Fig. 1. Workflow for selecting the seismic attribute to predict well log properties in well (Cynthia, 1997; Kalkomey, 1997).

*Corresponding author: atul.utp@gmail.com
[1]Note that PNN stands for Polynomial Neural Network (for mathematic) in this study. The abbreviation for Probabilistic Neural Network used in science and engineering is also PNN.

Table 1. Comparitive analysis of past techniques utilized to predict pseudo porostiy log from seismic attribute (Specht, 1990; Oh et al., 2001; Banchs, 2002; Dorrington et al., 2004; Singh et al., 2004; Choi, 2011; Hampson, 2011; Uden, 2013)

Technique used	CC Test	CC Training	Mean Testing Error (V/V)
Probabilistic Neural Network (PNN) using Multiattribute transform	0.86	0.95	0.037
Linear Multiattribute transform and Multilayer Feed Forward Neural Network (MLFN)	0.62	0.95	NA
Feed-forward back propagation Neural Network and Multivariate Linear Regression	0.62	0.82	0.026
Genetic Algorithm and Multilayer Feed Forward Neural Network (MLFN)	0.57	0.86	NA
Feed-forward back propagation Neural Network (FBPNN)	0.73	0.88	0.032
Polynomial Neural Network using GMDH (PNN*)	0.76	0.89	0.034

used to predict the reservoir properties away from the well control (Kalkomey, 1997; Balch et al., 1998).

The specificity and heterogeneity of the reservoir have a significant impact on the reservoir performance as they affect well productivity (Anderson, 1996; Alvan, 2011). Geophysicists determine seismic attributes as prognostic indicator of petrophysical properties of the reservoir (Gunning et al., 2006; Bakhshipour et al., 2013). Furthermore, its analysis reduces uncertainty for better correlation between well log and seismic response (Stephen et al., 2006; Moore et al., 2011). A nonlinear multivariable regression technique like Probabilistic Neural Network accompanied by stepwise regression, inversion, etc. has been utilized to correlate the seismic attribute statistically with reservoir properties (Kalkomey, 1997; Banchs et al., 2002). As illustrated in Table 1, nonlinear regression technique results in a better correlation coefficient ($r^2 = 0.82$) than a porosity model which is based on linear regression ($r^2 = 0.74$) (Banchs et al., 2002).

whereas, CC test and CC training are the average cross correlation coefficient for the test and training dataset respectively. The mean testing error defines the mean error within the generated and target datasets in case of testing (Valenti, 2009).

An implementation of multi-attribute and neural network analysis helps not only to generate pseudo log volume, but also integrate it with 3-D seismic and petrophysical properties of the reservoir (McLean et al., 2012). Furthermore, inversion of seismic data helps in predicting better correlation factor away from the well control as well as deals with generating the seismic reflectivity model (Todorov, 2000; Priezzhev, 2010). The logs are resampled at an interval of 2 ms to prevent an aliasing problem from the predicted synthetic seismogram during modeling (Fu et al., 1990; Taner et al., 1994). The reflection coefficient (RC) is computed using the following mathematical expression (Leite, 2011),

$$AI_M = AI_1 \exp(2\textstyle\sum_{j=2}^{M} r_j), \quad (1)$$

where, r_j is the reflection coefficient of the j^{th} layer and AI_1 and AI_M, are the acoustic impedances in the top and M^{th} layer, respectively.

Then, the source wavelet is convolved with the reflectivity series to generate a synthetic seismogram.

$$s_i(t) = \textstyle\sum_{j=1}^{N} r_j^*(t) w_{i-j+1}(t), \quad (2)$$

where, w(t), s(t) and r^* are the source wavelet, seismic trace and reflectivity, respectively.

The above methodology is a forward convolution of a reflective model with the estimated wavelet to generate synthetic seismogram similar to the desired seismic traces. The success of seismic inversion is critically based on an accurate estimation of wavelet's shape, which strongly influences the resultants of seismic inversion as well as assessments of the reservoir quality (Taner et al., 1994). Therefore, in order to estimate an accurate wavelet, seismic data traces by traces at well positioned are inverted to minimize the error between the predicted and true seismic traces.

In addition, seismic inversion is applied to estimate seismic impedance model from the resultant reflectivity model. Furthermore, on applying an empirical relationship between impedance and porosity, the estimated impedance log are converted into the predicted porosity log similar to true porosity log at measured wells. Such enhanced correlation factor helps in improving the prediction of reservoir properties.

2. METHODOLOGY

The improved inversion process has four main modules such as well log conditioning, seismic data conditioning, extraction of wavelet and low frequency modelling. As illustrated in Figure 7, the model has sub-modules which have their own significance.

These sub-modules are discussed and analysed separately by considering the key role of interpreter for making better decisions to select specific attribute for better reservoir modelling.

2.1. Conditioning of Well Log

Well logs are the physical mensuration of earth's properties, adopted among the enclosed space of a borehole. The variations in physical properties of reservoir such as depth, thickness, scale, grain distribution, etc. cause the borehole irregularities, poor parameter measurement or may cause loss of correct information (Stephen et al., 2006; Alvan, 2011).

Well logs data may be considered as a good indicator for rocks type and rocks properties while interpreting through seismic data. But the limitations of seismic data are its narrow bandwidth and resolution. Therefore, both well logs and seismic data are parameterized at different depth and time scales, which in turn cause better integration issue named dispersion effect (i.e., change in velocity due to frequency variation). Sonic log data are invariant to the borehole conditions, but its acquisition is performed at different length scales. On the other hand seismic data need dispersion correction for better tying to identity subsurface properties correctly. This will reinforce better reservoir modelling to understand the complete and reliable geology information (Jia et al., 2007).

Based on geological variation causing dispersion effect, it is necessary for consistency checking of rock physics variation by utilizing the rock physics model (Widuri, 2012). This model is capable of performing conversion of resultant parameters of reservoir simulation to its equivalent synthetic seismogram and is termed as forward seismic modeling. In addition, seismic parameters and its changes due to fluid saturation and variation in reservoir pressure have been estimated by using Gassmann's equations and the Hertz Mindlin model (Choi et al., 2011), respectively. Gassmann's equations give the saturated bulk modulus for each lithofacies and can be derived (Riazi et al., 2013; Uden et al., 2013).

$$K_{sat} = K_{dry} + \frac{\alpha^2}{\frac{\phi}{K_{fl}} + \frac{1-\alpha}{K_m}}, \tag{3a}$$

$$\alpha = 1 - \frac{K_{dry}}{K_m}, \tag{3b}$$

where, α = Volumetric constitutive constant associate with material drained and undrained response. ϕ = porosity, K_m = bulk modulus of the mineral. K_{fl} = fluid modulus and calculated by harmonic average of individual phase bulk moduli:

$$\frac{1}{K_{fl}} = \frac{S_w}{K_w} + \frac{S_o}{K_o} + \frac{S_g}{K_g}, \tag{4}$$

where, $S_{w,}$ is the water saturation and S_o, S_g is oil and gas saturations respectively. K_w is the water moduli and K_o, K_g is the oil and gas moduli respectively. These parameters are determined through laboratory analysis of field data and by utilizing the concept of primary thermodynamic properties equations (Riazi et al., 2013). K_{dry} is representing the bulk modulus of dry rock that can be derived from simulating the laboratory data. In addition, dry bulk modulus is derived from petroelastic transformation with suitable rescaling of experimentally measured parameters (Chen et al., 1997; Riazi et al., 2013). The measured bulk modulus is used with compliance (E_k) and stress at standard temperature and pressure (K_{inf}) to estimate dry bulk modulus as:

$$K_{dry} = \frac{K_{inf}}{1 + E_k \exp\left(-\frac{P_{eff}}{P_k}\right)}, \tag{5}$$

where, P_{eff} is effective pressure and the impedance for a column of cells in the simulation model is then calculated as:

$$I = \sqrt{\langle \rho \rangle \langle \frac{1}{M} \rangle^{-1}}. \tag{6}$$

In the above equation, ρ and M is defined as bulk density and P-wave moduli. The brackets < > indicate a vertical volume weighted average over the reservoir interval (Batzle et al., 1993). The resulting acoustic impedance is estimated by using the simple derived mathematical expression in Equation (1) which outcome is depicted in Figure 2. In order to determine the similarity of rock bodies at different locations, well data can be observed in well section window, which includes well header information such as Well name, Surface X, Surface Y, Kelly bushing (KB), Time-Depth (MD). The perfectly seismic-well tie requires domain conversion of well log data as it has depth domain, implemented by applying the velocity checkshot survey. Furthermore, time-depth calibration functions at control wells has been established so that surface-recorded seismic images can be reliably converted into the depth images that are needed to do reservoir volumetric calculations (Xu et al., 1995; Balch et al., 1998).

2.2. Seismic Quality Control

The analysis of seismic data provides ambiguous information about the geology. It requires the complete and accurate information about geophysical attributes of the reservoir. In addition, the relative amplitude for both well log and seismic data needs to be minimal during their acquisition and processing either vertically and spatially. This may help in determining the optimum parameters that derive the significant information of actual geology. In order to imaging the actual geology, it is necessary to optimize the stacking velocities properly to reduce velocity overflow (Banchs et al., 2002). However, proper migration is required to develop a geological model. It results in reducing variation in seismic amplitude with discontinuities which leads to improved seismic imaging. Some of the seismic attribute may be affected due to the variation in seismic wavelet, which cause variation in synthetic seismogram. In addition to this, signal to noise ratio error in the seismic data can be determined by mathematical operation, which is taken into consideration during the inversion process applied to the seismic data (Taner et al., 1979; Priezzhev, 2010). Likewise, some more seismic errors include; multiples, aliasing, etc. occurred, which cannot easily be quantified. In order to reduce these errors during the processing and to improve the inversion outcome, sampling and filtering is applied.

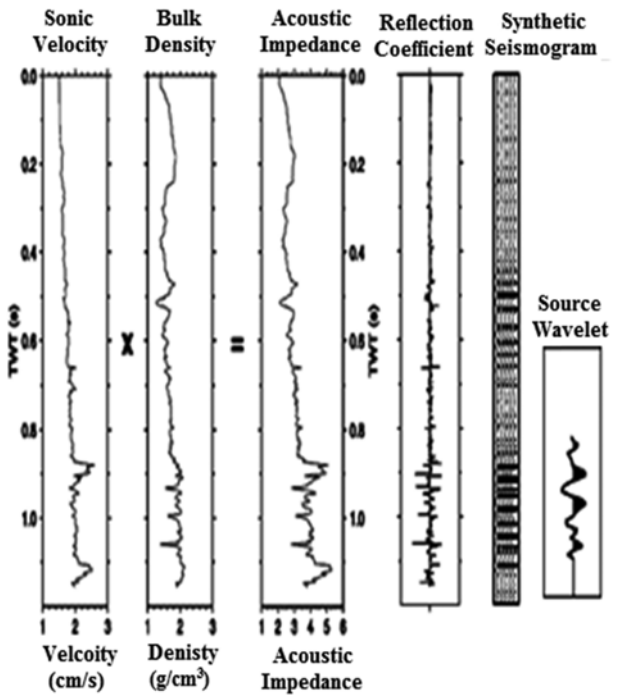

Fig. 2. Predicted reflection coefficient and synthetic seismogram after processing the data.

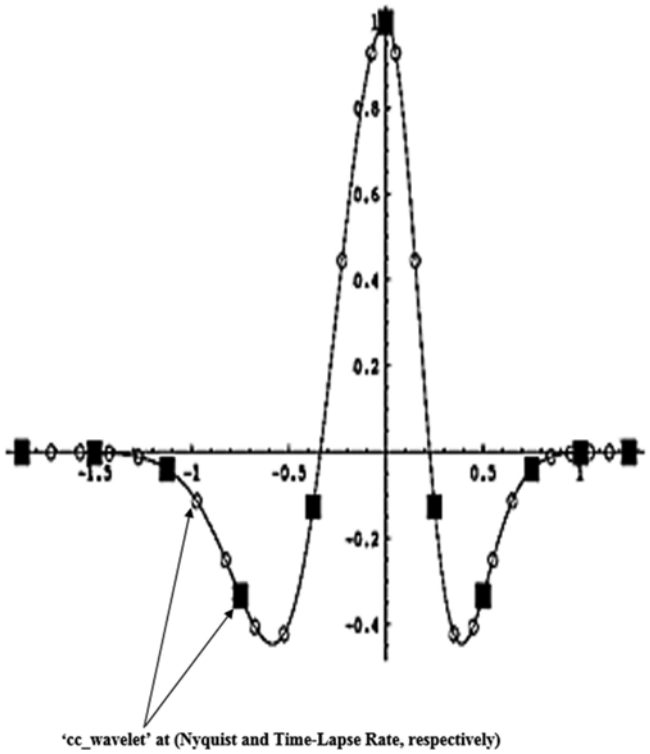

Fig. 3. Predicting RC and synthetic seismogram after extracting the wavelet coefficient ('cc_wavelet') at Nyquist rate (black boxes) and resultant coefficients at seismic time-sampling rate (circles) (James et al., 2006).

Based on the analysis of the predicted synthetic seismogram as shown in Figure 2, it is found that the reflectivity series starts immediately below the seafloor, which is excluded from the predicted synthetic seismogram. Furthermore, these traces are plotted with positive polarity so that positive reflections (increases in acoustic impedance) are plotted as black peaks. This convention has also been used in the display of the observed seismic data and has been repeated by five times (Fig. 2).

2.3. Wavelets

The wavelet is an impulse source response which determines the geophysical attributes while interpreting the seismic data. Wavelet may often derive from inversion of seismic data with a primary constraint such as well log data. But both types of data (sonic and density log) and seismic data are sensitive to errors due to variation in geological conditions (Dadashpour et al., 2009). To determine multi-well optimized wavelet, it is necessary to determine a wavelet at each well individually or collectively by considering each resultant wavelet and its associated errors.

To generalize the wavelet mathematically, the study considers a wavelet $w(a_w)$ parameterized by a set of coefficients a_w, with suitable prior $p(a_w)$. To determine priorities prior zeroes mean of the Gaussian dispersion method is utilized (James et al., 2006). In this each parameter of $w(a_w)$ is set to be as equispaced samples i = –M.....N (k_W in total). A Nyquist rate criterion is adopted for spacing the samples. It is the rate that directly linked with the seismic band edge (distinctly about $dt = 1/(4f_{peak})$) (Gunning et al., 2006).

$$\tilde{w} = w(a_w)\,. \tag{7}$$

The seismic traces s (t) is generated when the reflectively and compact wavelet is known. The better resultant seismogram is generated when the wavelet is zero phases (Fig. 3). It determines the true source signature in the geology (derived from seafloor or salt-top reflections, or perhaps even impulsive source from the explicit modeling). Inversely to cross-correlated the resultant wavelet, reflectivity of the earth can be determined by deconvolution of the seismic data (Taner et al., 1994; Dadashpour et al., 2009). The whole inversion processing of seismic data helps to characterize an 'effective' wavelet, which is more symmetrical and compact than the actual source signature.

3. SONIC CALIBRATION WORKFLOW

Sonic calibration is the process of creating the synthetic sonic log which is utilized to match with true well logs (Fig. 4). In addition, seismic data are imported after applying the domain conversion process on imported well log data. Moreover, the velocity checkshots are applied on well and seismic data to establish the depth-time calibration between

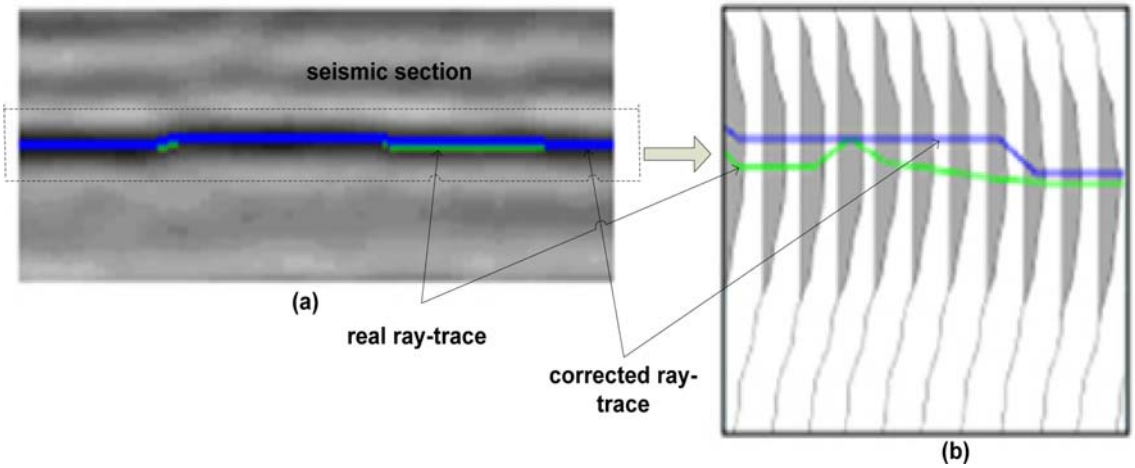

Fig. 4. Sonic calibration by knee point (time shift) using nearest peak. (a) Real seismic image; (b) Enlarge section of highlighted portion in Figure 4a.

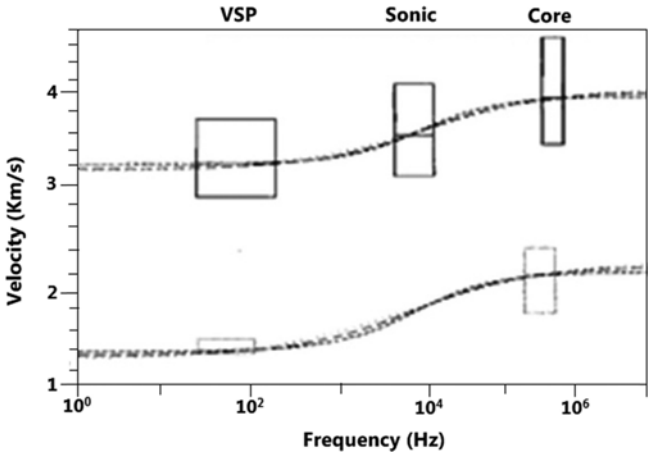

Fig. 5. Compressional and shear wave velocity dependency on frequency. The dotted line is showing S-waves (Sams et al., 1997).

well and seismic data (Xu et al., 1995). This results in computing the seismic velocity, acoustic impedance and signature for the synthetic logs.

3.1. Wavelet Extraction to Generate Synthetic Seismogram

It is obvious that the generation of synthetic seismogram is based on perfect seismic-well tie. For the purpose, selection of a better wavelet is necessary to establish the linking between the well log and seismic data. The complete study of rocks physical model also evidences that rocks are dispersive in nature. This will result a fact that seismic velocity almost always increases with increasing frequency such that: Core > Sonic > Crosshole > Vsp > Seismic.

Therefore, in this approach various types of wavelets at variant frequency are extracted by using the wavelet extraction process as shown in Figure 6. The type of wavelet, frequency (Hz) used, and sampling and scaling factors are defined as:

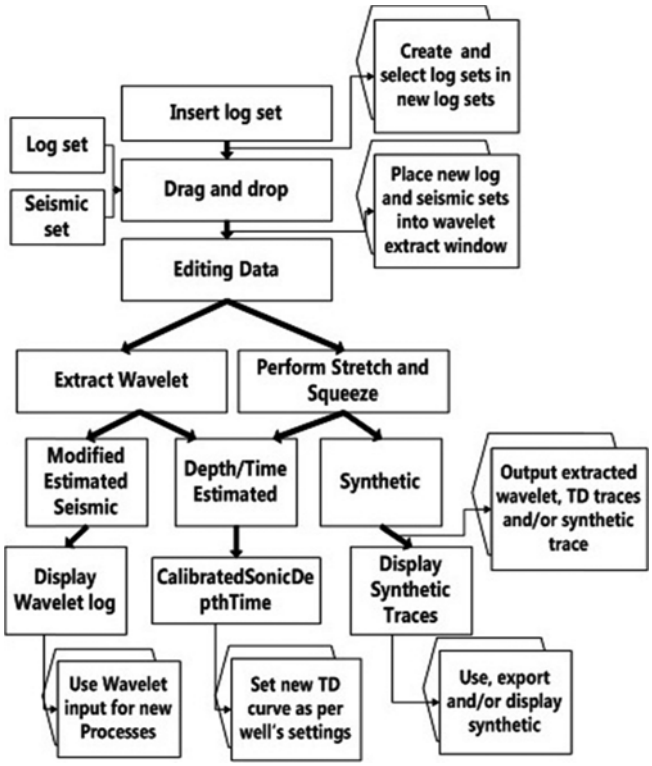

Fig. 6. Wavelet extraction workflow.

(i) Ricker wavelet having frequency (f), 20 Hz, Sample 2 ms, Scale 128 ms.

Ricker wavelet having frequency (f), 30 Hz, Sample 2 ms, Scale 126 ms.

$$A = (1-2\pi^2 f^2 t^2)e^{-\pi^2 f^2 t^2}. \quad (8)$$

Ormsby wavelet having frequencies f_1, f_2, f_3 and f_4, such as low cut (10 Hz), low pass (20 Hz), high pass (50 Hz), hig cut (70 Hz), Sample (2 ms), Scale (128 ms).

$$A = \left[\frac{(\pi f_i)^2}{\pi f_i - \pi f_{i-1}}\mathrm{sinc}^2(\pi f_i t) - \frac{(\pi f_{i-1})^2}{\pi f_i - \pi f_{i-1}}\mathrm{sinc}^2(\pi f_{i-1} t)\right]$$

$$- \left[\frac{(\pi f_{i-2})^2}{\pi f_{i-2} - \pi f_{i-3}}\mathrm{sinc}^2(\pi f_{i-2} t) - \frac{(\pi f_{i-3})^2}{\pi f_{i-2} - \pi f_{i-3}}\mathrm{sinc}^2(\pi f_{i-3} t)\right], \quad (9)$$

where, A is the amplitude of the Ricker wavelet with peak frequency f at time t in both the Equations (8) and (9).

Based on the extracted parameters such extracted wavelet as shown in (Figs. 9a and b) are convolved with extracted reflection coefficients to generate synthetic log. From the analysis, it is found that Ormbsy bandpass wavelet shown better matching result than synthetic log created by convolving reflection coefficients with Ricker wavelet.

4. LOW FREQUENCY MODELLING

The low frequency model (LFM) is represented as constrained sparse-spike inversion workflow, which considers the dispersion effect and filling the frequency gaps from the zero to low level of the seismic bandwidth. The filling of the gap is followed in such a way that the filled data is matched with well log data. Such correlated resultant data become an indicator to determine geophysical attributes. Based on derived data analysis, prominent impedance image (having cutting inversion side-lobes) is obtained with resultant inversion quantitatively (e.g., reliable porosities or fluid prediction) (Hampson et al., 2001). However the error is still propagated with the resultant data due to the large variation in amplitude and phase of the traces in the data, causing discontinuity, which led to changes in phase spectrum and may cause variation in modelled geology. In order to overcome this issue, a model derivation of the horizon must be smoothened where less variation in geology takes place. Such picking of horizon in the designed model help in reducing geologic discontinuities (e.g., faults). Furthermore, consistency of Cartesian product of the horizons of the derived model results in improving the scaling of well log data at seismic location which helps in sampling the data easily and cause fewer multiples (Tonn et al., 2002). In order to build the modelled geology, an interpreter analyses each sub-step of the whole designed low frequency model to minimize the error.

Therefore, this paper introduces a model for achieving the current and future objectives. In order to achieve these objectives, the whole model can be divided into two parts: (i) Low frequency modelling and (ii) Polynomial Neural Network (PNN*) based mathematical modelling for training the correlated attribute to generate pseudo log volume while applying on the whole seismic volume as shown in Figure 7.

According to the Figure 7, two types of data sets are taken into account in this model (well-log and seismic) with the

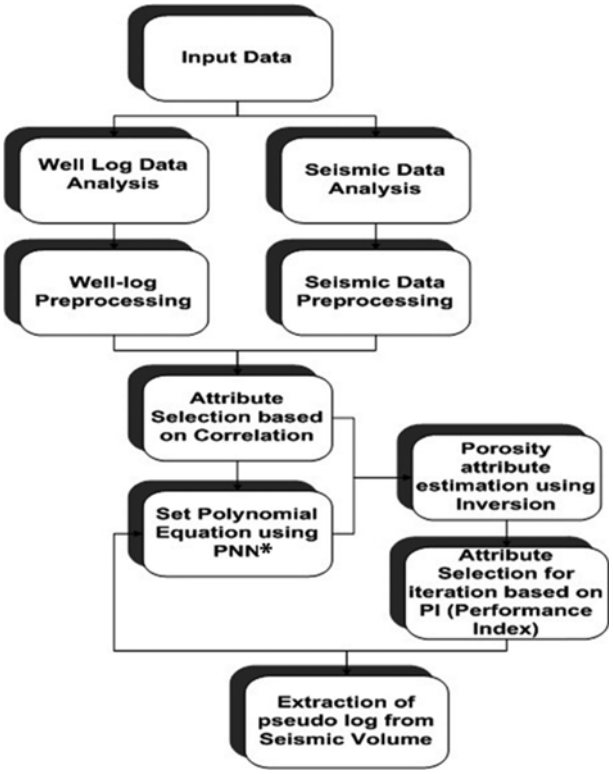

Fig. 7. Mathematical model for estimation of pseudo log volume.

following steps of constructions.

Step1: All well logs are changed from depth-to-time by using Time-Depth curves after sampling.

Step2: (i) Performing resampling of resultant data from step1 with the spline interpolation.

(ii) It makes the data uniformly spaced similar to sampled seismic data.

Step3: (i) Ormsby bandpass filter is used to avoid aliasing problems during the downsampling of log data by the limit of their spectral content.

(ii) After that resample the log data at uniform interval to preserve its resolution.

Step4: (i) Performing upsampling the seismic data in order to match log samples.

(ii) Matching results in attribute selection from the well log and seismic data.

Step5: Training procedure is done using PNN over selected attributes to set the polynomial equation by using the estimated selected weights.

Step6: (i) Extract correlation weights from the set polynomial equation in step5 by implementing inversion procedures.

(ii) Final correlated weights (attributes) are then implemented on whole seismic volume to produce pseudo log volume.

4.1. Logic of PNN*

Polynomial Neural Network (PNN*) is elastic in struc-

ture (topology) which is governed by the Group method of data handling (GMDH) learning based approach (Farlow, 1981; Oh et al., 2001). PNN* utilizes a number of regression polynomial structures such as linear, bilinear, modified quadratic, cubic, etc. The processing of PNN* makes it a self-organizing multi-layered iterative network for determining better partial description (PDs). Such computed PDs are further analyzed to determine the best correlated partial description (PDs) by selecting definite number of network layers and correlated seismic attribute.

The optimization feature of PNN* is to improve the time and running complexity of the model based on the data requirement. The aimed approach of PNN* includes:

• To generate the best external partial descriptions (correlated attribute) from selected PDs (attributes) at each layer. The decision of further iteration and the addition of the network layer is based on resultant PDs to reach at best correlation.

• Generation of best partial description (PDs) by selecting significant correlated attributes and order of the polynomial.

Relation of data set as Input-output defined as follows:

$$(X_i Y_i) = (X_{1i}, X_{2i}, \ldots, X_{ni}, y_i), i = 1, 2, \ldots, m, \quad (10a)$$

$$n = n_{tr} + n_{tc}, \quad (10b)$$

where, n_{tr}, n_{tc} are the size of training and testing data sets.

Estimated Output read as:

$$\hat{y} \text{or} \phi = \hat{f}(x_1, x_1, \ldots, x_N) = a_0 + \sum_{i=1}^{N}(b_i x_i) + \sum_{i=1}^{N}(c_{ij} x_i x_j) + \sum_{i=1}^{N}(d_{ijk} x_i x_j x_k) + \cdots, \quad (11)$$

where, a_0, b_i, c_{ij}, d_{ijk}, are the coefficients of polynomials and the number of polynomial coefficients may vary depending upon the order and the number of layers in the polynomial neural network.

In the present research, noise associated with the seismic data during acquisition causes random errors with higher complexity in it called issue of over-fitting (Liu et al., 1999). Therefore, the whole data is distributed into some variable percentage of training and testing dataset (see Fig. 8) with the feature that both are composed of a well-log sample and its related seismic attribute samples, such that:

$$x = (\underbrace{x_{1i} + \cdots + x_{nti}}_{\text{Training}})\ (\underbrace{x_{nti+1} + \cdots + x_n}_{\text{Testing}}),$$

$$y = (\overbrace{y_{1i} + \cdots + y_{nti}})\ (\overbrace{y_{nti+1} + \cdots + y_n}).$$

Here, model constructing new variables such as z_1, z_2, z_3, …, $z\binom{m}{2}$. Based on the equation model, all the independent variables (i.e., column of array X) such as x_1, x_2, x_3,…, x_m are considered for computing partial description (PDs). From each X variable two pairs are considered at a time and for each $\binom{m}{2}$ least square polynomial is determined which have the form as:

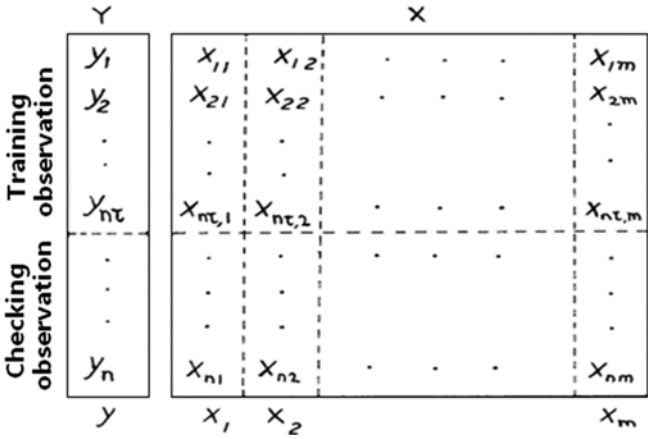

Fig. 8. Modeling showing differentiation of training and testing datasets.

$$y = A + Bx_1 + Cx_2 + Dx_1^2 + Ex_2^2 + Fx_1x_2. \quad (12)$$

For each pair of x_1, x_2…x_n, data point are defined as (x_{11}, x_{12}), (x_{21}, x_{22}),…, (x_{n1}, x_{n2}) and each data point will replace the first column of Z based on the computed PD's. This process is continuing iteratively until all the data points are converted into the new polynomial variables of the form z.

4.2. Polynomial Neural Network Algorithm for LFM

The Polynomial neural network is a self organizing algorithm which is based on the group method of data handling (GMDH), where number of layers is dynamic and variated as shown in Figure 9. The number of iterative layers in PNN* depends upon the expected resultant PDs.

The PNN* algorthim is define as:

Step 1: Determine the number of seismic attributes to processing as x_i, i = 1,2, ……., N.

(a) For selecting Advanced PNN*: set of less than three attribute value is iterative.

(b) For selecting Generic PNN*: set of more than three attribute value is iterative.

Step 2: Generate a Training and Testing datasets to estimate correlation using Equation (10b).

Step 3: Selecting the structure of PNN* on the basis of selected order of the polynomial.

(a) Simple type PNN* structure.

(b) Modified type PNN* structure.

Step 4: Determine the order of a polynomial and number of correlated attribute to generate Partial description from trained datasets.

Step 5: Compute the correlation coefficients based on selecting PDs.

Step 6: Performing iteration to determine better correlated PDs at best predictive capability.

Step 7: Checking the stopping and additional criterion for next new layer and iteration.

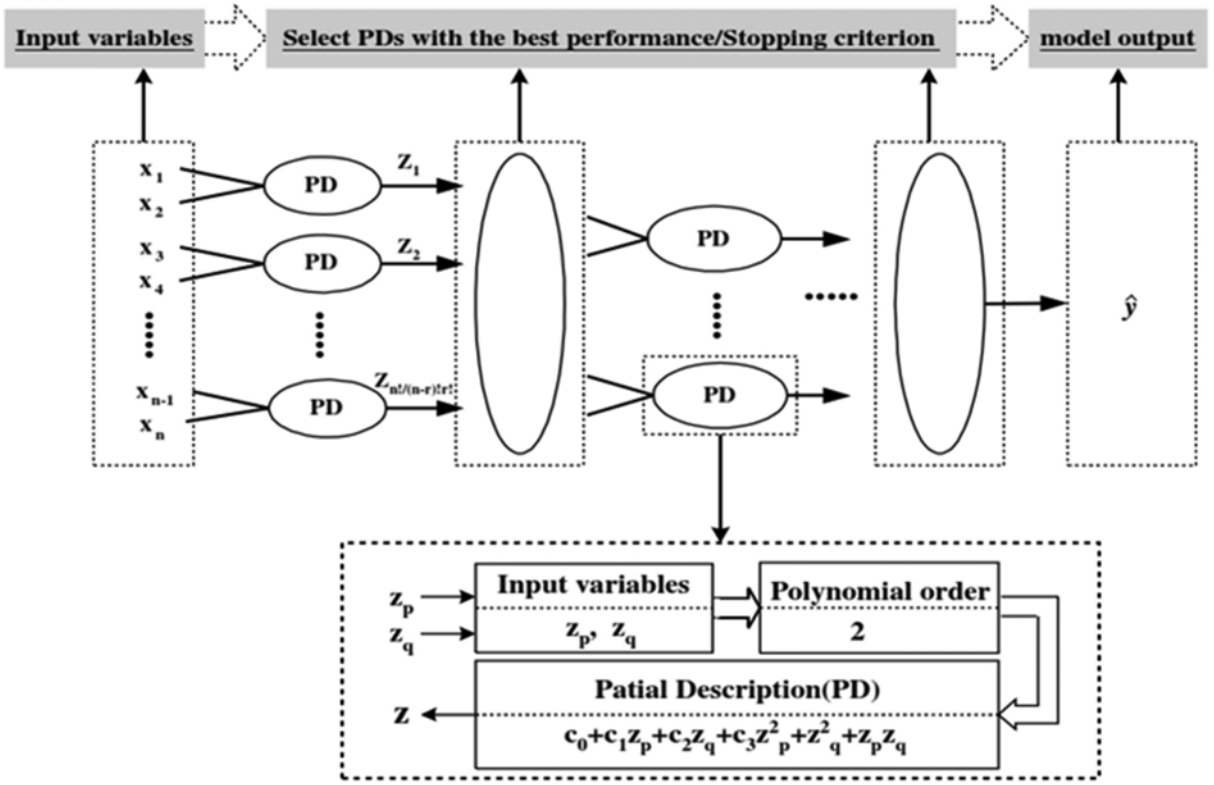

Fig. 9. Polynomial neural network (PNN*) model.

$$E_j \geq E_*, \tag{13}$$

where, E_j = Minimal computing error at current layer of the network.

E_* = Minimal computing error occurring at the previous layer of the newtork.

Step 8: Determine new input attributes for the next iterative layer as new PDs variable as:

$$x_{1i} = z_{1i}, x_{2i}, z_{2i}, \ldots, x_{ni} = z_{ni}. \tag{14}$$

Such that, the total number of PDs sited at the present layer is differing from the total number of a selected number of correlated attributes at the preceding layer, such that:

$$\text{Nodes (or PDs): } k = N!(N-r)!r!, \tag{15}$$

where, r = Number of selecting attribute at present iterative layer.

However, the best selection of PDs is based on the better correlation coefficients C_i. Whereas, the vector of C_i is computed by optimizing the mean squared error between y_i and z_{mi}.

$$E = \frac{1}{N_{tr}} \sum_{i=1}^{N_{tr}} (y_i - z_{mi}). \tag{16}$$

So, coefficients are only determined using N_{tr} (Training dataset). Therefore, by using the training dataset, a set of linear equation gives rise:

$$Y = X_i C_i. \tag{17}$$

Eventually, the coefficients of the PD of nodes in each layer are expressed in the form as:

$$C_i = (X_i^T X_i)^{-1} X_i^T Y, \tag{18a}$$

$$Y = [y_1\ y_2 \ldots y_{ntr}]^T, \tag{18b}$$

$$X_i = [X_{1i}\ X_{2i} \cdots X_{ki} \cdots X_{ntri}]^T, \tag{18c}$$

$$X_{ki}^T = [1\ x_{k1i}\ x_{k2i} \cdots x_{kin} \cdots x_{ki1}^m \cdots x_{kin}^m], \tag{18d}$$

$$C_i = [C_{0i}\ C_{1i}\ C_{2i} \cdots C_{ni}]^T, \tag{18e}$$

where, i = Node number in the layer processed, k = Subset data number processed, n_{tr} = Number of Training datasets, n = Number of choosing correlated attribute, m = Maximum polynomial order, n' = Number of computed coefficients.

Hence, the processing of PNN* results in a trained set of attributes that is capable of computing a better correlation coefficient between the well log and seismic data. Such trained parameters are further applied on the whole seismic volume to generate pseudo log volume which would help in improving the reservoir characterization by providing information about petrophysical properties both near and away from the well log. In addition, proposed low frequency model

would also help in depicting the better reservoir definition, prediction and performance.

5. RESULTS AND DISCUSSION

The better reservoir characterization requires complete information of petrophysical properties of subsurface both near and away from the well control. Integration of well logs (measured at depth) and surface seismic (measured at two-way time) data provides interpreted horizons and true phases of surface seismic. Such integration process results in generation of synthetic seismogram, which act as an indicator for identifying multiples on the surface seismic. In order to obtain accurate synthetic seismogram, it requires better calibration of sonic

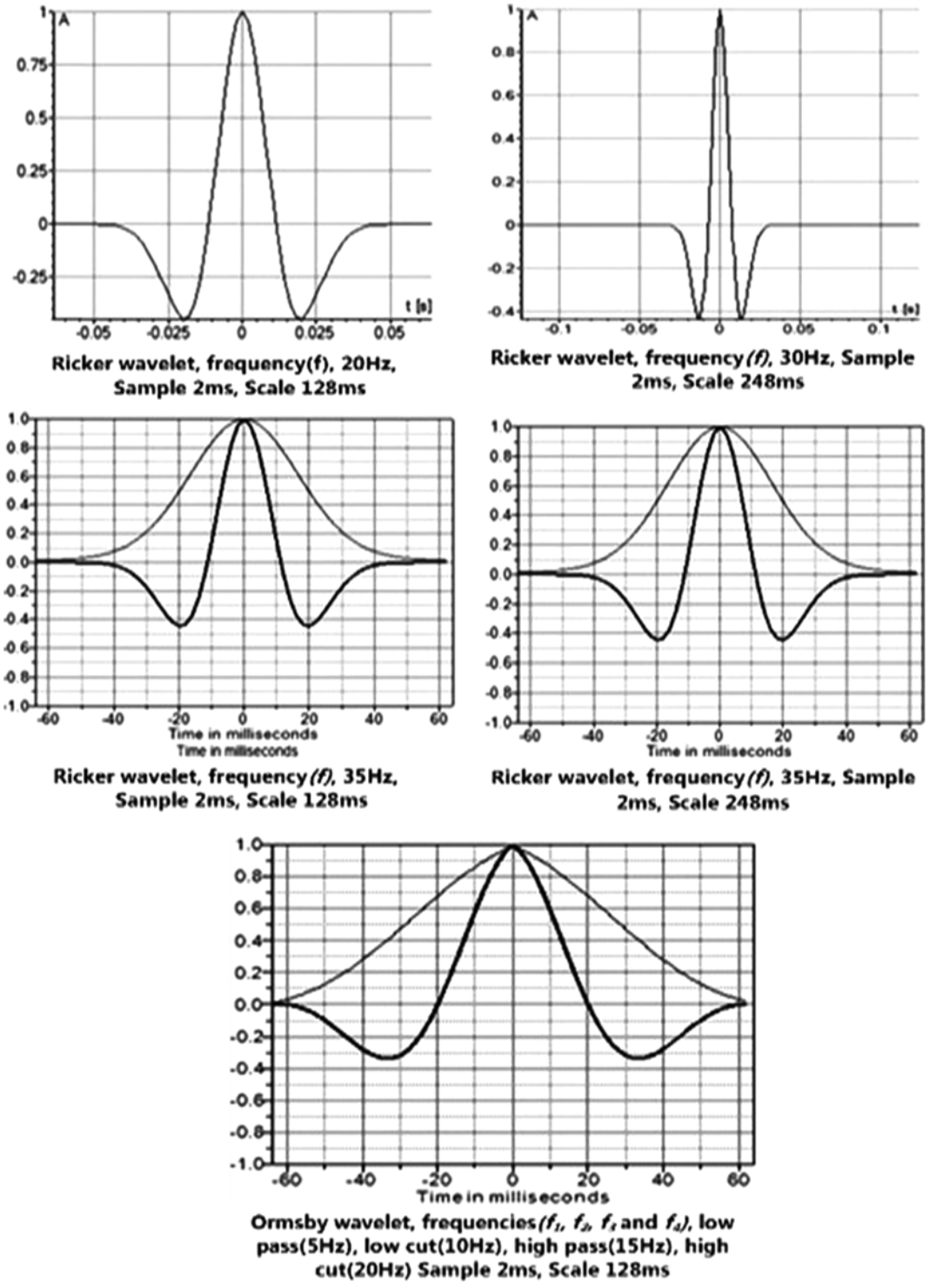

Fig. 10. (a) Wavelet extracted from surface seismic data after sonic log calibration.

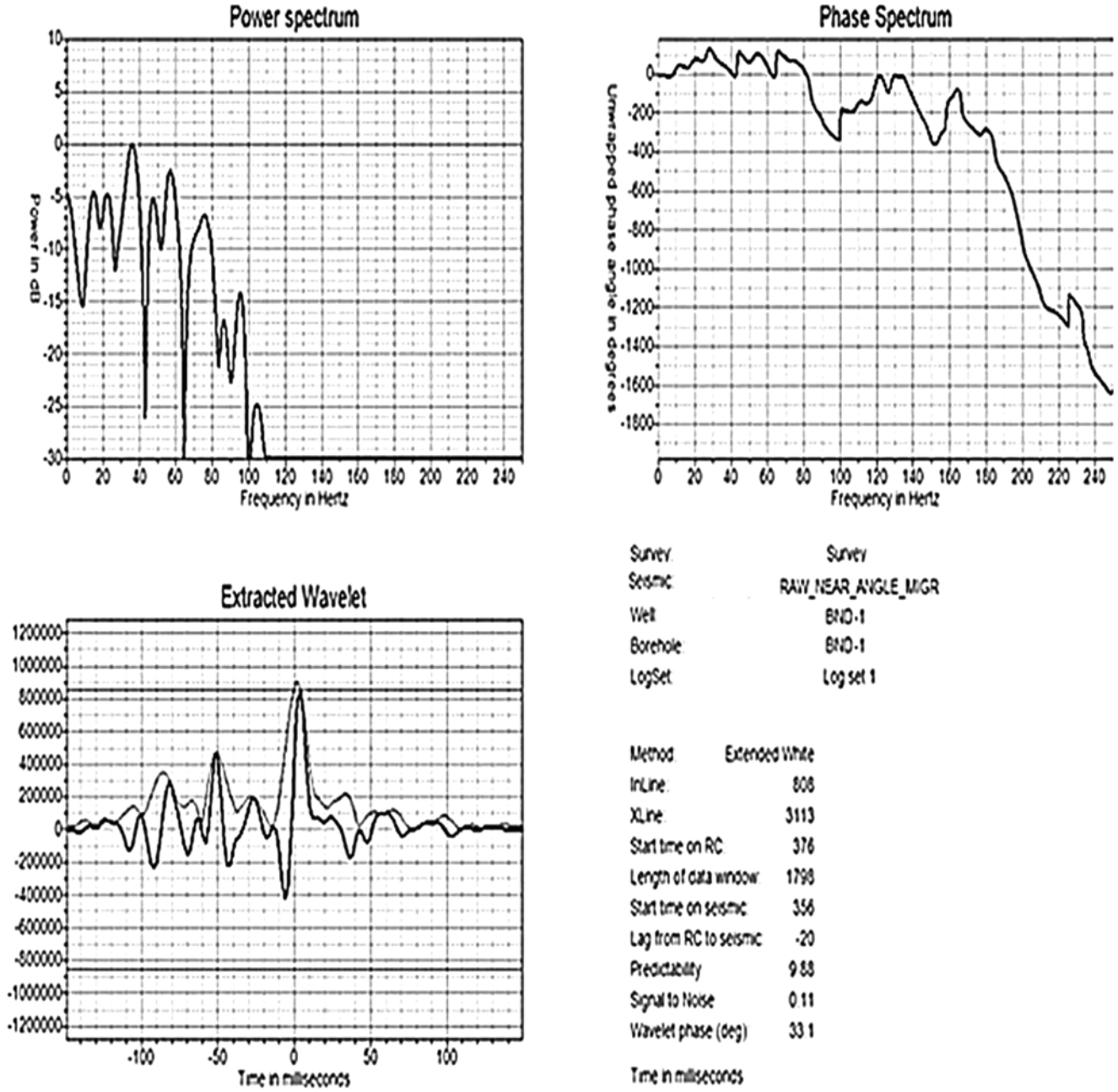

Fig. 10. (continued) (b) Wavelet extracted from surface seismic data after sonic log calibration.

logs by utilizing vertical seismic profile or velocity checkshot survey. The implementation of calibration is necessary because of the fact that:

i. Sampling of sonic log and surface seismic at variant frequency (Dispersion effect shown in Fig. 5).

ii. Measurement of different fluid volumes and rock type from the well logs and seismic data. Such variations are referred as:

(a) Invaded zones,

(b) Fluid differences,

(c) Damaged borehole,

(d) Non-vertical ray paths, etc.

The result of such calibration represents the scaling of both the data such that the timing of sonic log and surface seismic data matches at "more accurate agreement (up-scaled) as shown in Figure A1 in (Appendix 1). Such sampling result helps in converting precisely the corrected sonic logs into an interval velocity. Additionally, acoustic impedance is calculated by multiplying the corrected velocity with rock bulk density by adjusting the algebraic expression mentioned in Equation (1) (see Figs. 2 and A2 (Appendix 2)). Such resultant AI values are utilized to determine the reflectivity time series

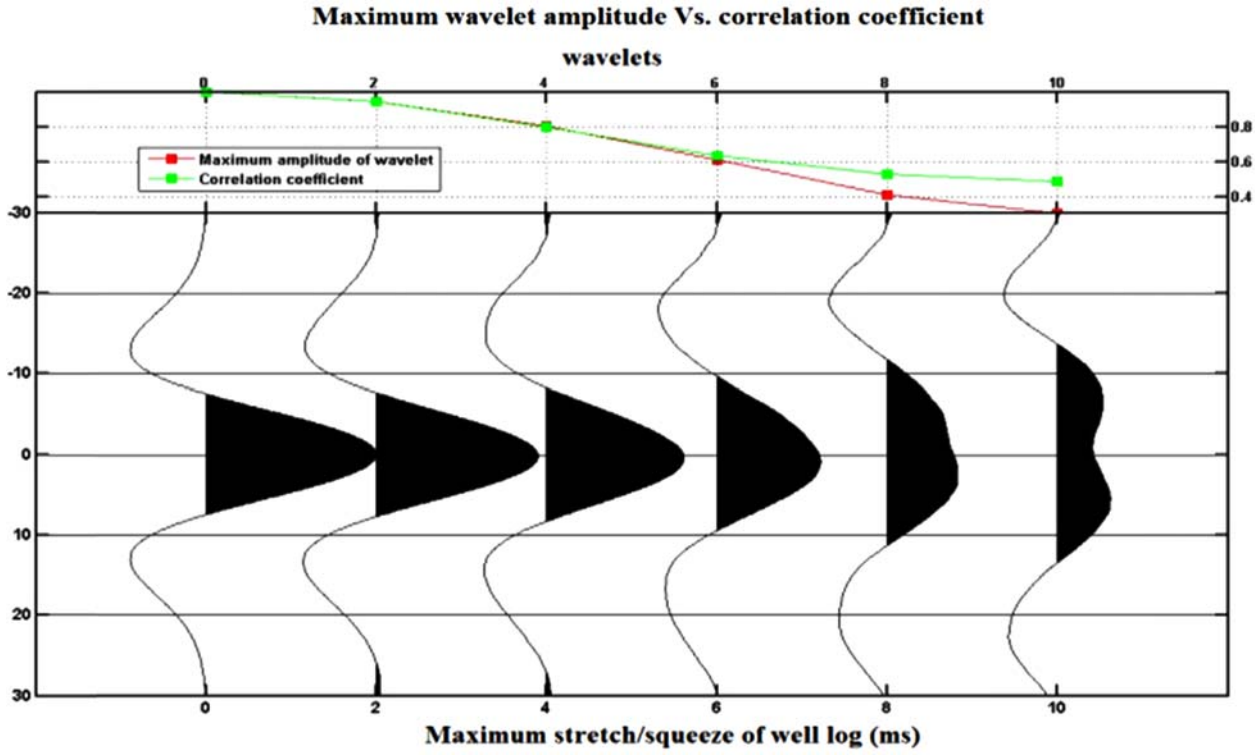

Fig. 10. (continued) (c) Plot seismic headers 'max' (maximum wavelet amplitude) and 'cc_wavelet' (cross-correlation between seismic and synthetic) above the wavelets.

or reflection coefficient (RC) by implementing the reflective seismogram equation as shown in Figure 11. This reflectivity time series (RC) is further convolved with determined wavelet to generate the synthetic traces. A better extraction of wavelets and its phase is necessary to generate feasible synthetic seismogram to achieve a better correlation coefficient between the predicted and true seismic traces. Therefore, the estimation of a wavelet from the well log and seismic data is approached in two ways:

i. Wavelet extracted from the seismic data after applying sampling for scaling both types of data.

ii. Synthetic wavelet is extracted at variant frequencies and of two types such as Ricker wavelet (Eq. 8) and Ormsby wavelet (Eq. 9).

Based on the analysis of variation in phase and amplitude of resultant wavelet, it can be concluded that each extracted wavelet has significant variation with relative correlation coefficient when cross-correlate with the predicted and true seismogram as shown in Figure 10c.

Moreover, convolution of such resultant wavelet with RCs results in variation in the predicted seismogram and its computed correlation coefficient while cross-correlate with the true seismic traces at well position. Therefore, the results based on such analysis signified that Ormsby wavelet has minor correlation than Ricker wavelet while cross-correlate with the predicted and true seismic traces as shown in Figures 11 and 12a–c.

In order to achieve a better seismic-well tie, it is necessary to have a feasible match/correlation between the predicted and true seismic traces. Therefore, after extraction of variant synthetic seismogram while convolution with different type of wavelet, it is required to perform iteratively stretching/squeezing of the predicted traces. In addition, relative velocity shift with velocity picking is performed to match the synthetic with real seismogram. The outcome showed better seismic-well tie that lead to achieving a higher correlation coefficient between the predicted and true seismic traces (Fig. 13). Also, it is analyzed from the results that Ricker wavelet at a 30–35 Hz frequency shows a better matching between the synthetic and true seismic traces even at high resolution and high amplitude as well as low resolution and low amplitude of RCs. Therefore, it can be concluded that the resultant synthetic seismogram showed a higher correlation when cross-correlated with true seismic that leads to better reservoir define, prediction and performance.

6. CONCLUSION

Accurate reservoir characterization requires complete information of petrophysical properties of reservoir both near and away from the well logs. It will help in reducing geological uncertainties to model the reservoir properties accu-

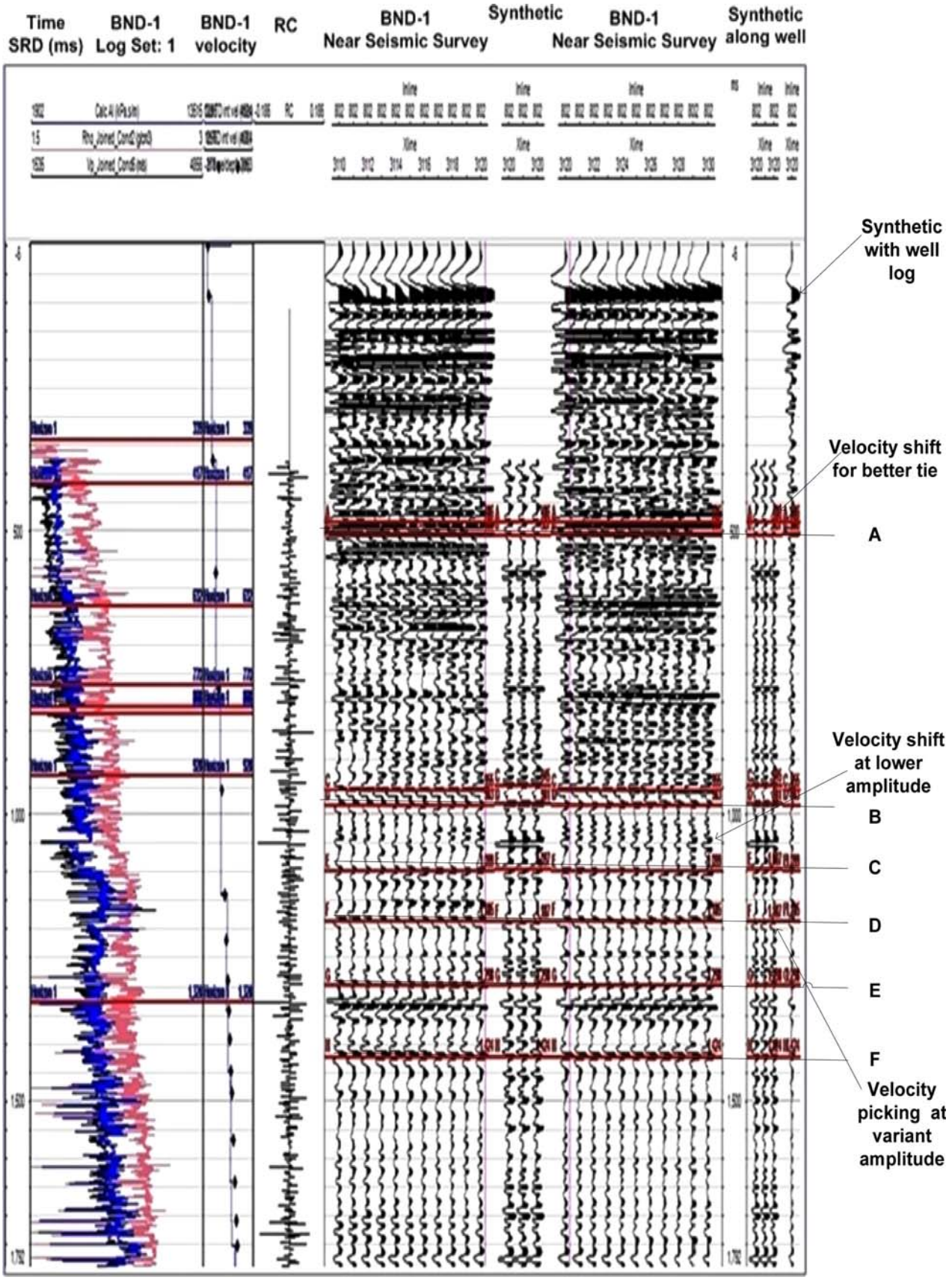

Fig. 11. Wavelet extraction from seismic.

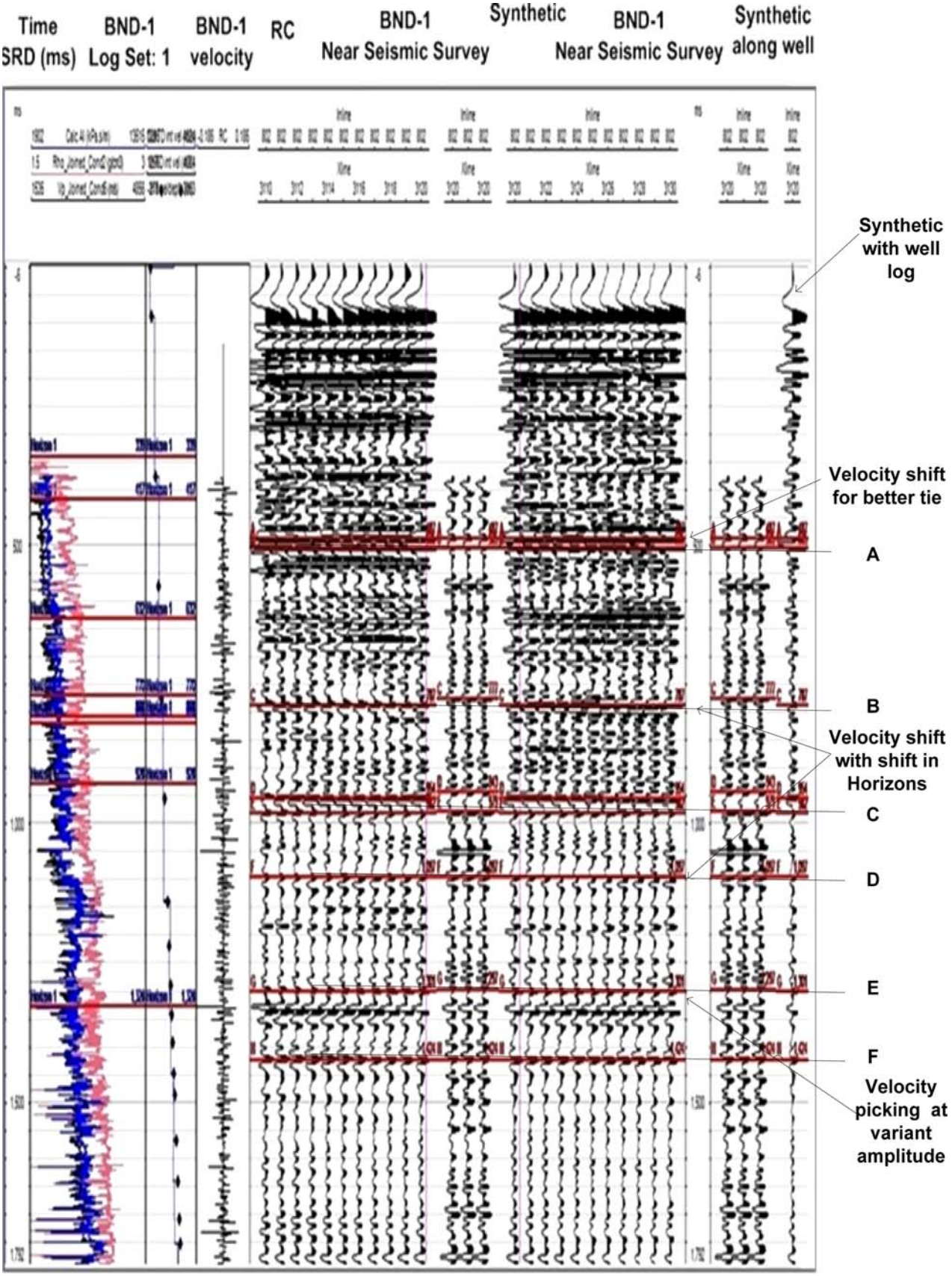

Fig. 12. (a) Synthetic seismogram when RC convolved with Ricker (30 Hz) wavelet.

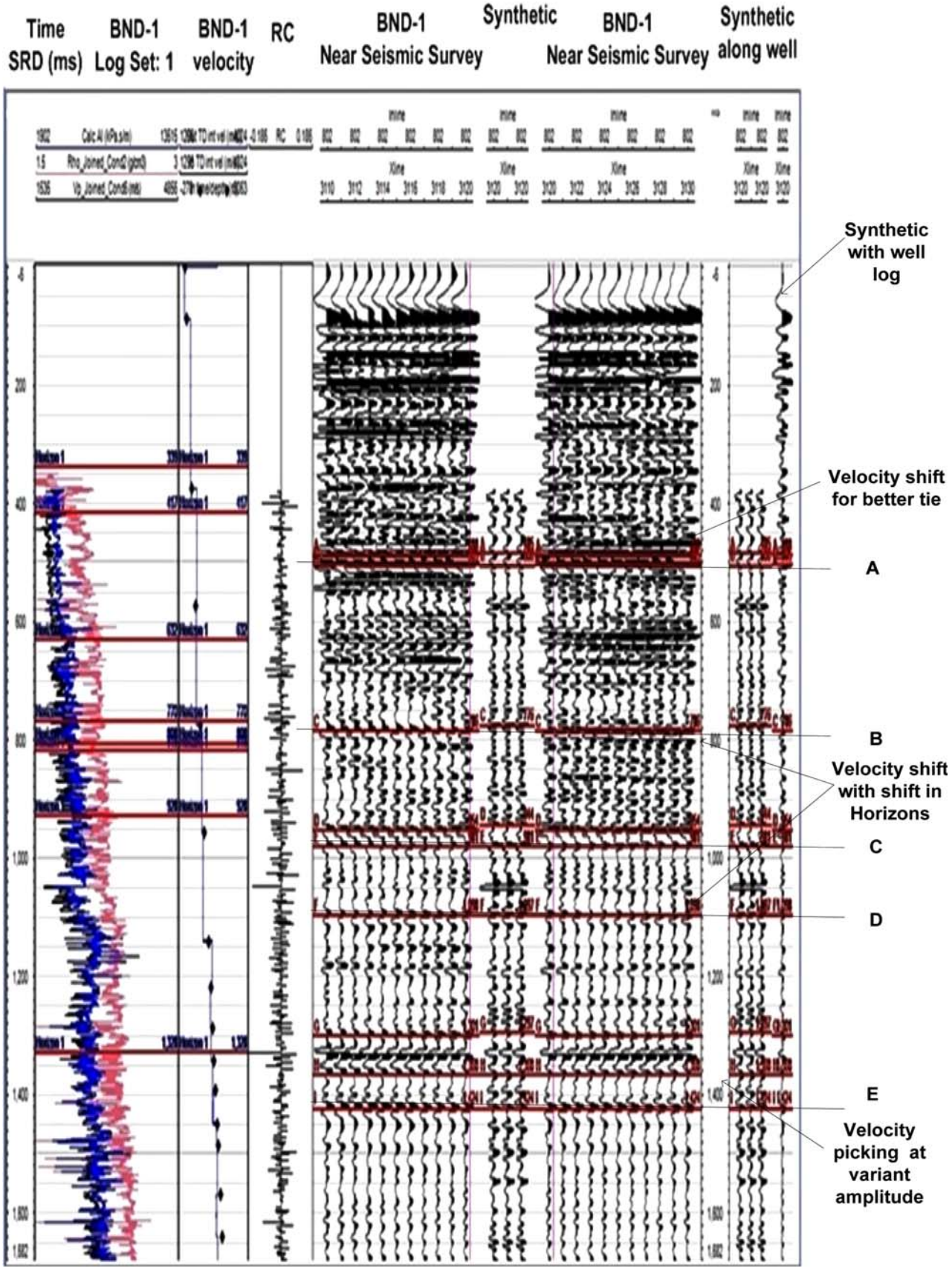

Fig. 12. (continued) (b) Synthetic seismogram when RC convolved with Ormsby wavelet.

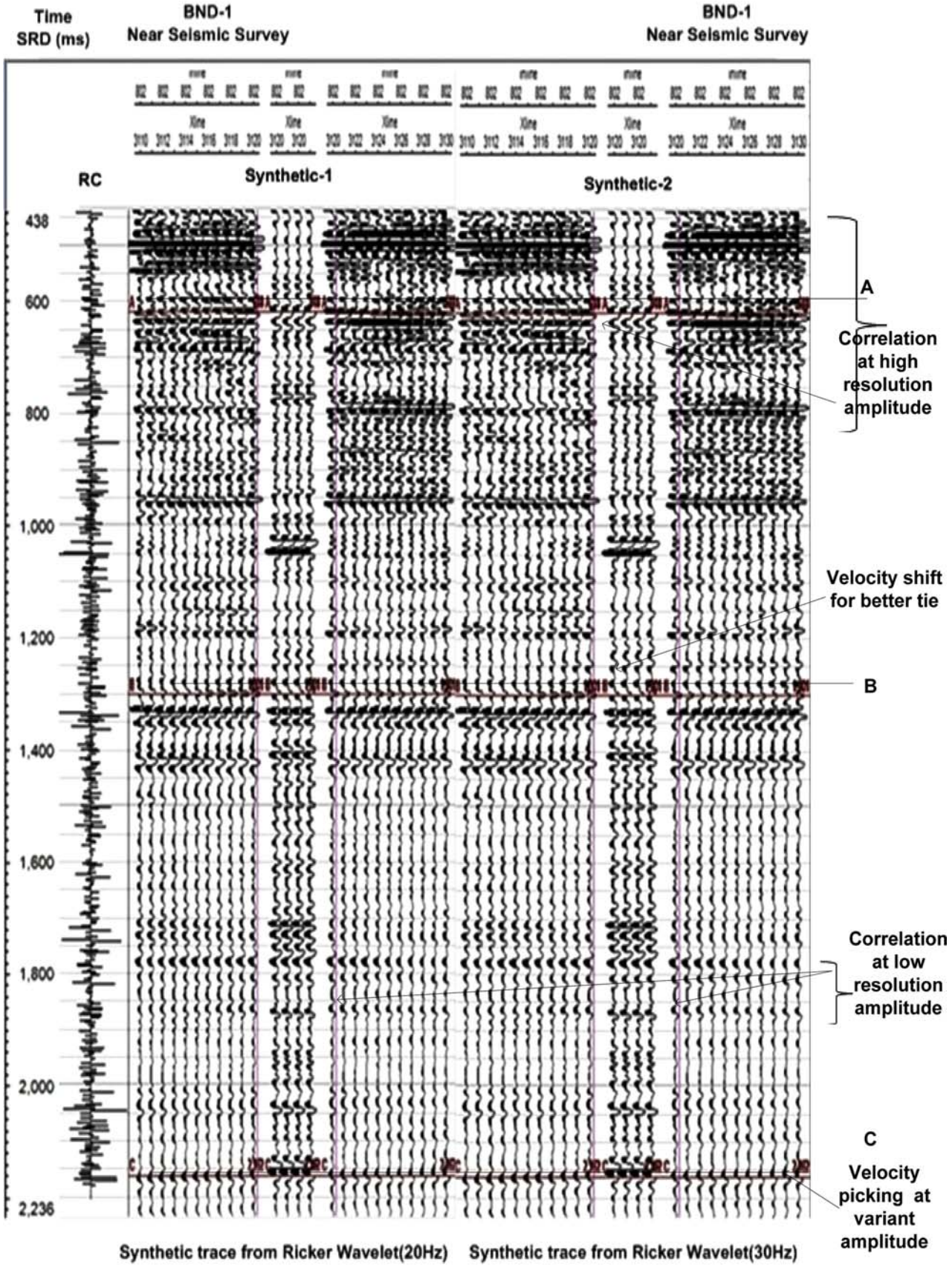

Fig. 12. (continued) (c) Synthetic seismogram when RC convolved with Ricker wavelet at different in frequency.

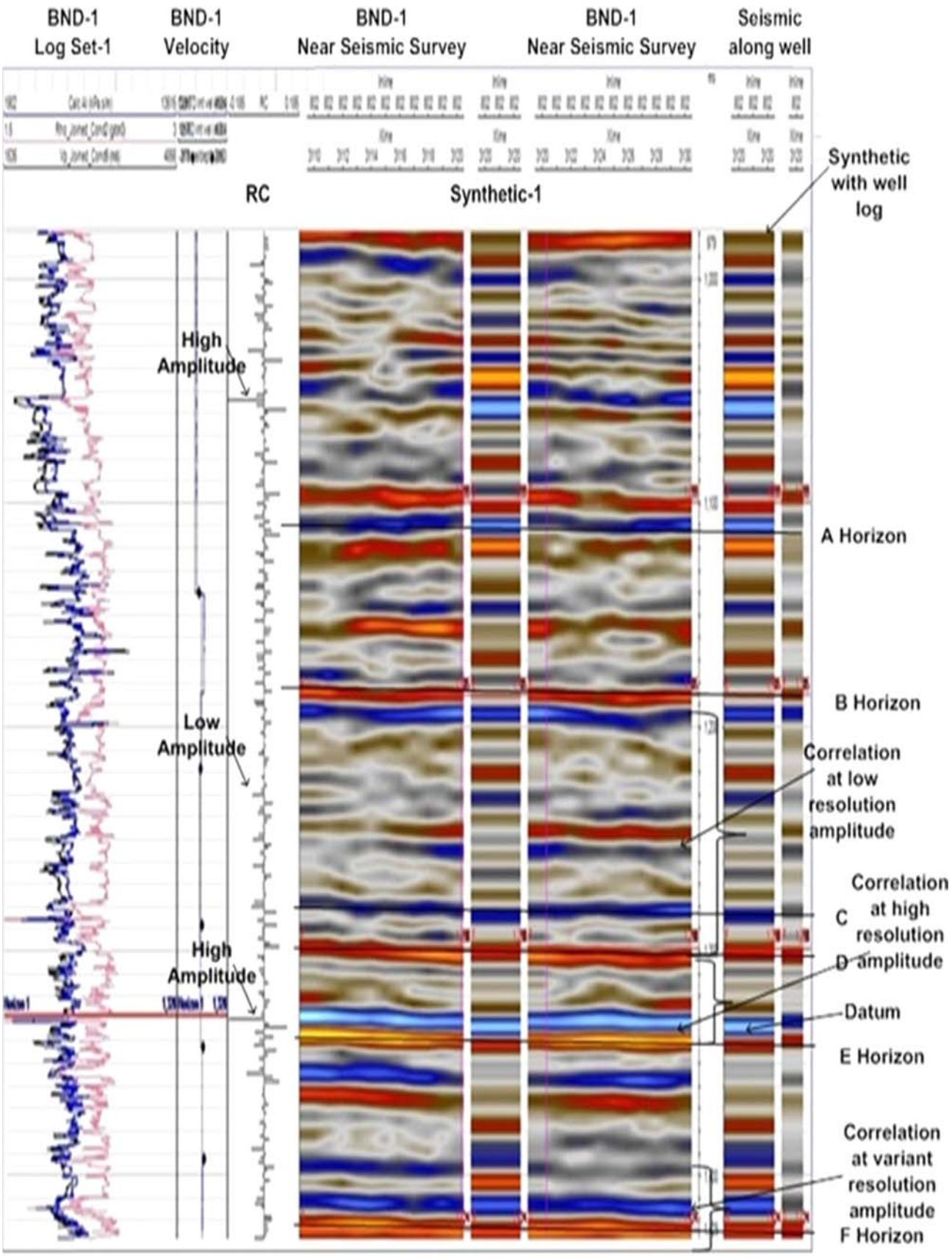

Fig. 13. Resultant of seismic-well tie showing matched zone.

rately. Compared to pre-existing techniques, a self-organizing learning based polynomial neural network (PNN*) algorithm is useful to generate a low frequency model. PNN* provides a better correlation coefficient (r^2) than linear modelling because of its optimized network feature and better runtime complexity.

The critical point for pre-existing techniques is the generation of a better synthetic seismogram by performing seismic-well tie. It results in a poor correlation coefficient between the predicted and true seismic traces due to the existence of multiples and aliasing problems in the data. Therefore, a precise upscaling of both types of data is performed in the designed model in order to overcome this issue. Such sampling data helps in extracting a more accurate wavelet which results in a feasible seismic-well tie. Furthermore, seismic inversion adopted in the designed model helps in extracting a higher correlated seismic attribute from the predicted traces. By utilizing the PNN* over the resultant correlated attributes, a trained LFM model is proposed to generate a pseudo log volume that are similar to true log volume. The achieved higher correlation helps in improving the reservoir characterization that leads to a better estimation of hydrocarbon resources. This model would also provide an accurate reservoir modeling at low frequency by utilizing a minimum number of measured wells.

ACKNOWLEDGMENTS: This work is supported by the YUTP project (Ref: YUTP-FRG/1/2012/EOR/039) by PETRONAS Sdn Bhd, Malaysia, and URIF project (Ref: URIF 12/2012) by Universiti Teknologi PETRONAS, Malaysia.

REFERENCES

Alvan, H.V., 2011, Uncertainty of estimated petrophysical parameters of Ahvaz oil reservoir. Journal of Advanced Science and Engineering Research, 1, 165–176.

Anderson, J.K., 1996, Limitations of seismic inversion for porosity and pore fluid: lessons from chalk reservoir characterization and exploration. 66th Annual Meeting of Society of Exploration Geophysicists (Expanded Abstract), Denver, Nov. 10–15, p. 309–312.

Bakhshipour, Z., Huat, B.K., Ibrahim, S., Asadi, A., and Kura, N.U., 2013, Application of geophysical techniques for 3D Geohazard mapping to delineate cavities and potential sinkholes in the northern part of Kuala Lumpur, Malaysia. The Scientific World Journal, Article ID 629476. doi:10.1155/2013/629476 2013.

Balch, R.S., Weiss, W.W., and Wo, S., 1998, Correlating seismic attributes to reservoir properties using multivariate non-linear regression. Proceedings of the West Texas Geological Society Fall Symposium, Midland, Oct. 29–30, p. 199–203.

Banchs, R.E. and Michelena, J., 2002, From 3D seismic attributes to pseudo-well-log volumes using neural networks: practical considerations. The Leading Edge, 21, 996–1001.

Batzle, M. and Wang, Z., 1992, Seismic properties of pore fluids. Geophysics, 57, 1396–1408.

Chen, Q. and Sidney, S., 1997, Seismic attribute technology for reservoir forecasting and monitoring. The Leading Edge, 16, 445–50.

Choi, J.W., Byun, J.M., and Seol, S.J., 2011, Generation of pseudo porosity logs from seismic data using a polynomial neural network method. Journal of the Korean Earth Science Society, 32, 665–673.

Dadashpour, M., Ciaurri, D.E., Kleppe, J., and Landr, M., 2009, Porosity and permeability estimation by integration of production and time-lapse near and far offset seismic data. Journal of Geophysics and Engineering, 6, 1–32.

Dorrington, K.P. and Link, C.A., 2004, Genetic-algorithm/neural-network approach to seismic attribute selection for well-log prediction. Geophysics, 69, 212–221.

Farlow, S.J., 1981, The GMDH algorithm of Ivakhnenko. American Statistician, 35, 210–215.

Fu, Q., Horvath, S., Potter, E., Roberts, F., Tinker, S.W., Ikonnikova, S., Fisher, W., and Yan, J., 2013, Log-based thickness and porosity mapping of the Barnett Shale Play, Fort Worth Basin, Texas: A proxy for reservoir quality assessment. Presented at the US Association for Energy Economics Workshop on Unconventional Gas and Oil, Austin.

Gunning, J. and Glinsky, M.E., 2006, Wavelet extractor: A Bayesian well-tie and aavelet extraction program. Computers & Geosciences, 32, 681–95.

Hampson, D., Schuelke, J.S., and Quirein, J.A., 2001, Use of multiattribute transforms to predict log properties from seismic data. Geophysics, 66, 220–236.

Jia, T.Y., 2007, Characteristics of sedimentary facies and reservoir properties of some tertiary sandstone in Sabah and Sarawak, East Malaysia. M.Sc. Thesis, Universiti Sains Malaysia, Penang, 42 p. (in English with Malay abstract).

Kalkomey, C.T., 1997, Potential risks when using seismic attributes as predictors of reservoir properties. The Leading Edge, 16, 247–251.

Leiphart, D.J. and Hart, B.S., 2002, Case history: Comparison of linear regression and a probabilistic neural network to predict porosity from 3-D seismic attributes in Lower Brushy Canyon channeled sandstones, southeast New Mexico. Geophysics, 66, 1349–1358.

Leite, E.P., 2010, Seismic model-based inversion using Matlab. In: Leite, E.P. (ed.), Matlab-Modelling, Programming and Simulations, Vol. 1: Computer Science and Engineering. Sciyo, InTech, 19, p. 405–412.

Liu, Z.P. and Castagna, J.P., 1999, Avoiding overfitting caused by noise using a uniform training mode. International Joint Conference on Neural Networks (Expanded Abstract), Washington, D.C., July 10–16, 3, p. 1788–1793.

McLean, J.K., Dulac, J.C., and Gringarten, E., 2012, Integrated Petrophysical Uncertainty Evaluation Impacts Reservoir Models. HART ENERGY, Exploration & Production. http://www.pdgm.com/resource-library/articles-and-papers/2012/integrated-petrophysical-uncertainty-evaluation-im/.

Moore, W.R., Ma, Y.Z., Urdea, J., and Bratton, T., 2011, Uncertainty analysis in well-log and petrophysical interpretations. American Association of Petroleum Geologists Memoirs, 96, 17–28.

Oh, S.K. and Pedrycz, W., 2001, The design of self-organizing polynomial neural networks. Information Sciences Association for Computing Machinery Digital Library, 141, 237–258.

Oh, S.K., Pedrycz, W., and Park, B.J., 2001, Polynomial neural networks architecture: Analysis and design. Computers & Electrical Engineering, 29, 703–725.

Priezzhev, I.I., 2010a, Prestack and poststack seismic inversion workflow in frequency domain. 4th International European Association of Geoscientists and Engineers Conference (Extended Abstract), Saint Petersburg, April 5–8, B24.

Riazi, N., Lines, L., and Russell, B., 2013, Integration of time-lapse seismic analysis with reservoir simulation. GeoConvention 2013:

Integration, 61–66.
Sams, M.S., Neep, J.P., Worthington, M.H., and King, M.S., 1997, The measurement of velocity dispersion and frequency-dependent intrinsic attenuation in sedimentary rocks. Geophysics, 62, 1456–1464.
Singh, V.B., Negi, S.P.S., Subrahmanyam, D., Biswal, S., and Baid, V.K., 2004, Generation of pseudo-log volumes from 3D seismic multi-attributes using neural networks: A case study. 5th Conference and Exposition on Petroleum Geophysics, Hyderabad, Jan. 15–17, p. 541–549.
Specht, D.F., 1990, Probabilistic neural networks. Neural Networks, 3, 109–118.
Stephen, K.D., Soldo, J., Macbeth, C., and Christie, M.A., 2006, Multiple model seismic and production history matching: A case study. Society of Petroleum Engineers Journal, 11, 418–430.
Taner, M.T., Koehler, F., and Sheriff, R.E., 1979, Complex seismic trace analysis. Geophysics, 44, 1041–1063.
Taner, M.T., Schuelke, J.S., O'Doherty, R., and Baysal, E., 1994, Seismic Attributes Revisited. 64th International Annual Meeting of Society of Exploration Geophysicists (Expanded Abstracts), Los Angeles, Oct. 23–28, p. 1104–1106.
Todorov, T.I., 2000, Integration of 3C-3D seismic data and well logs for rock property estimation. M.Sc. Thesis, University of Calgary, Calgary, 94 p.
Tonn, R., 2002, Neural network seismic reservoir characterization in a heavy oil reservoir. The Leading Edge, 21, 309–312.
Uden, R.C., Smith, M., and Hubert, L., 2003, Neural network training for reservoir characterization of litho facies. 65th European Association of Geoscientists and Engineers Conference and Exhibition, Stavanger, June 2–5, p. 99.
Valenti, J.C., 2009, Porosity prediction from seismic data using multiattribute transformations, N Sand, Auger Field, Gulf Of Mexico. M.Sc. Thesis, The Pennsylvania State University, University Park, 84 p.
Widuri, I., 2012, Seismic multi-attributes analysis to predict lithology distribution and porosity. 74th European Association of Geoscientists and Engineers Conference and Exhibitions (Expanded Abstracts), Copenhagen, June 4–7, p. 1–4.
Xu, S. and White, R.E., 1995, A new velocity model for clay-sand mixtures. Geophysical Prospecting, 43, 91–118.

Manuscript received December 1, 2014
Manuscript accepted July 7, 2015

APPENDIX 1: Results after performing sonic calibration during Seismic-well tie

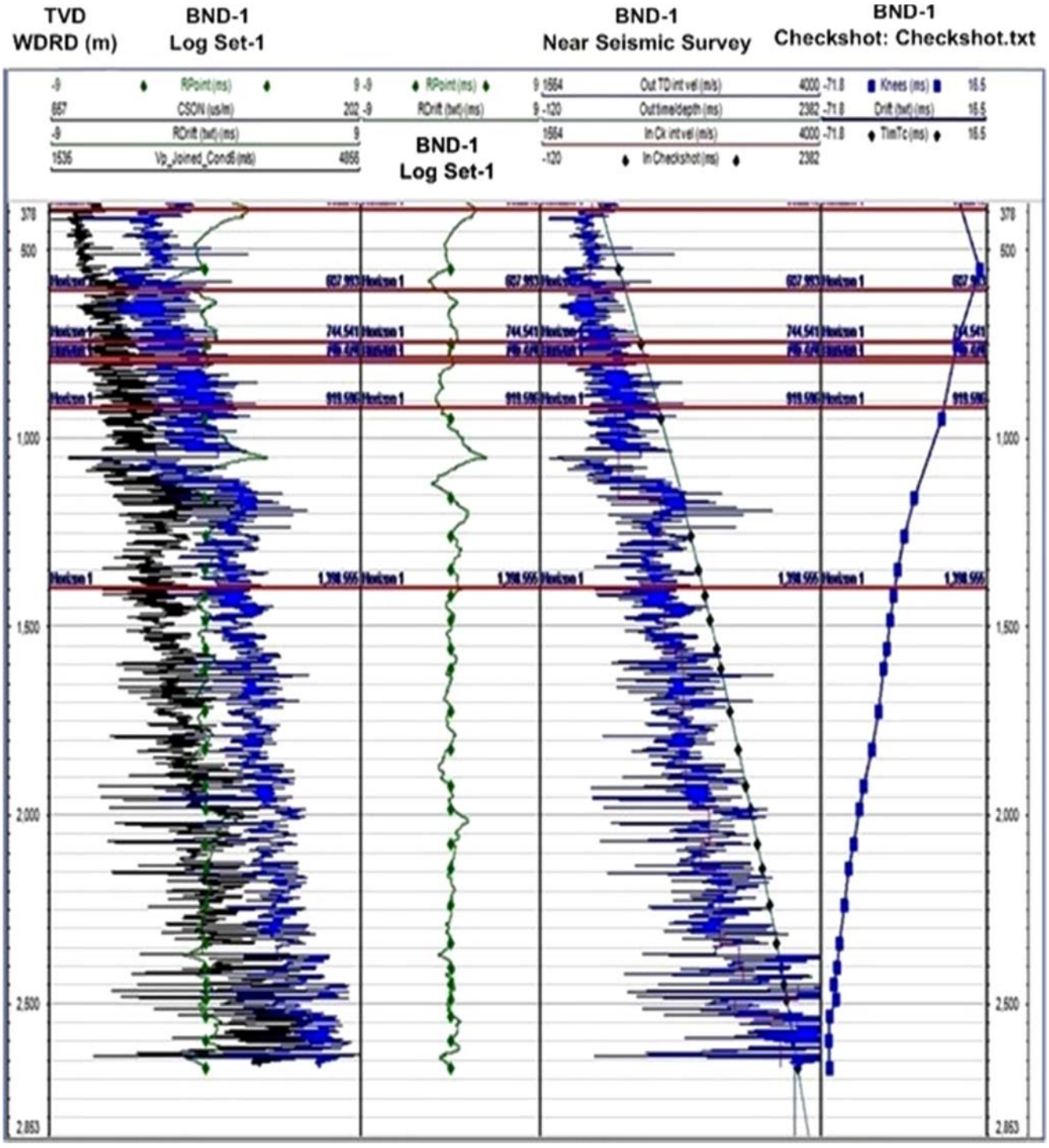

Fig. A1. Interpolated resulant after sonic calibration.

APPENDIX 2: Result after performing Seismic forward modeling

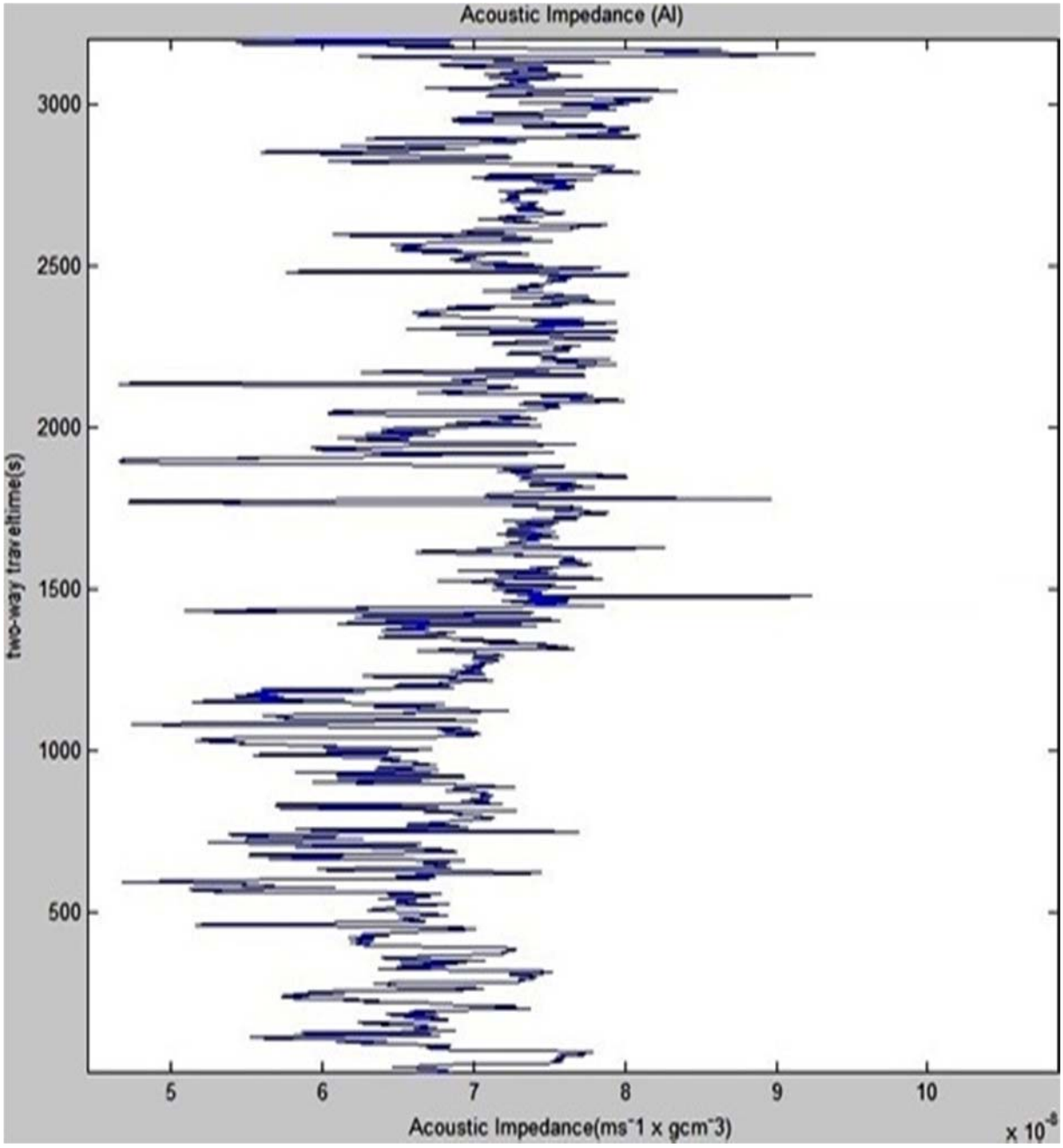

Fig. A2. Calculated acoustic impedance from the well log data.